

# Transport, multifractality, and the breakdown of single-parameter scaling at the localization transition in quasiperiodic systems

Jagannath Sutrardhar, Subroto Mukerjee, Rahul Pandit, and Sumilan Banerjee

*Centre for Condensed Matter Theory, Department of Physics, Indian Institute of Science, Bangalore 560012, India*



(Received 18 November 2018; revised manuscript received 6 April 2019; published 18 June 2019)

There has been a revival of interest in localization phenomena in quasiperiodic systems with a view to examining how they differ fundamentally from such phenomena in random systems. Motivated by this, we study transport in the quasiperiodic, one-dimensional Aubry-Andre model and its generalizations to two and three dimensions. We study the conductance of open systems, connected to leads, as well as the Thouless conductance, which measures the response of a closed system to boundary perturbations. We find that these conductances show signatures of a metal-insulator transition from an insulator, with localized states, to a metal, with extended states having (a) ballistic transport (one dimension), (b) superdiffusive transport (two dimensions), or (c) diffusive transport (three dimensions); precisely at the transition, the system displays subdiffusive critical states. We calculate the  $\beta$  function  $\beta(g) = d \ln(g)/d \ln(L)$  and show that, in one and two dimensions, single-parameter scaling is unable to describe the transition. Furthermore, the conductances show strong nonmonotonic variations with  $L$  and an intricate structure of resonant peaks and subpeaks. In one dimension the positions of these peaks can be related precisely to the properties of the number that characterizes the quasiperiodicity of the potential; and the  $L$  dependence of the Thouless conductance is multifractal. We find that, as dimension increases, this nonmonotonic dependence of  $g$  on  $L$  decreases and, in three dimensions, our results for  $\beta(g)$  are reasonably well approximated by single-parameter scaling.

DOI: [10.1103/PhysRevB.99.224204](https://doi.org/10.1103/PhysRevB.99.224204)

## I. INTRODUCTION

The single-parameter scaling theory of Abrahams *et al.* [1] has played an important part in our understanding of Anderson localization and metal-insulator transitions in disordered systems, e.g., noninteracting electrons in a random potential [2]. Localization phenomena are, however, not only restricted to random systems, but also occur in other systems, the most prominent examples being systems with quasiperiodic potentials [3–11]. Recently such quasiperiodic systems have attracted a lot of attention because of the experimental observation of many-body localization (MBL) in quasiperiodic lattices of cold atoms [12]. These have brought back into focus the need to examine the essential similarities and differences between random and quasiperiodic systems at the level of eigenstates [3–11], dynamics [13–15], and universality classes of localization-delocalization transitions [16]. It has also been argued [16] that quasiperiodic systems provide more robust realizations of many-body localization (MBL) than their random counterparts because the former do not have rare regions, which are locally thermal. Therefore, we may find a stable MBL phase in dimension  $d > 1$  in a quasiperiodic system, but not in a random system, where the MBL phase may be destabilized because of such rare regions [17,18].

Noninteracting quasiperiodic systems exhibit delocalization-localization transitions even in one dimension, unlike random systems in which all states are localized in dimensions  $d = 1$  and  $2$  for orthogonal and unitary symmetry classes [19]. The simplest rationale for the absence of a metallic (delocalized) state in low-dimensional

random systems and the continuous nature of the localization-delocalization transition in three dimensions is provided by the single-parameter-scaling theory [1], which has been proposed originally for random systems. This theory relies on only a few general premises: (a) there is a length( $L$ )-dependent, dimensionless conductance,  $g(L) = G(L)/(e^2/h)$ ; (b) there is a single relevant scaling variable such that  $d \ln(g)/d \ln(L) = \beta(g)$  depends only on  $g$ ; (c) there is a continuous and monotonic variation of  $\beta(g)$ , with well-known asymptotic behaviors for small and large conductances. Even though the conductance  $g(L)$  of a finite system (a) fluctuates strongly and (b) is a non-self-averaging quantity [20–22], a large number of numerical studies [23–25] have provided the justification for the single-parameter scaling theory, at least in a weak sense [26] for typical or average conductances [24–26]. Hence, to distinguish quasiperiodic systems from random ones, it is natural to ask whether there is a single-parameter-scaling description of the delocalization-localization transition in quasiperiodic systems or whether quasiperiodic systems do not satisfy one or more of the assumptions of the scaling theory. This question is particularly relevant now because a recent study [27] suggests that the delocalization-localization transition in a three-dimensional (3D), self-dual, quasiperiodic model is in the same universality class as the conventional 3D Anderson transition in a random system. Hence, we might expect, naïvely, that single-parameter scaling holds, at least, for this class of 3D quasiperiodic systems. We examine this naïve expectation in detail.

Some recent works [13–15] have examined open-system transport and closed-system wave-packet dynamics in quasiperiodic chains, described by the Aubry-Andre model [3] and its variants [28,29], and have shown that the delocalization-localization critical point exhibits anomalous behavior: An initially localized wave packet spreads diffusively or superdiffusively with time in an isolated system, whereas the conductance, at high or infinite temperature, shows subdiffusive scaling with system size, i.e.,  $g \sim L^\alpha$  with  $\alpha < -1$ , for open chains connected, at its ends, to two infinite leads [13,14]. These results indicate that quasiperiodic systems have much richer transport properties, at this critical point, than random systems.

Motivated by the above, we ask the following questions: (a) How similar are the transport properties of quasiperiodic and random systems, especially at the metal-insulator transition? (b) Is there a simple scaling theory for this transition in quasiperiodic systems along the lines of the seminal, single-parameter-scaling theory for random systems [1]? (c) What is the dimension dependence of such transport properties at the metal-insulator transition in quasiperiodic systems? (d) Are the Thouless and Landauer conductances the same in quasiperiodic systems?

To answer these questions, we carry out a systematic characterization of electronic transport in the quasiperiodic, 1D Aubry-Andre model and in its 2D and 3D generalizations. We study the (Landauer) conductance of open systems connected to leads as well as the Thouless conductance, which is a property of a closed system. Our main results, which address all the above questions, are the following:

(1) We show that, depending on the dimension  $d$ , the Thouless and Landauer conductances show signatures of the insulator-metal transition from an Anderson insulator to (a) a ballistic metal in one dimension, (b) a superdiffusive metal in two dimensions, or (c) a metal with diffusive transport in three dimensions. Precisely at the transition, the system displays subdiffusive critical states.

(2) We calculate the  $\beta$  function  $\beta(g) = d \ln(g)/d \ln(L)$  and show that, in one and two dimensions, the  $\beta$  function is discontinuous at the transition and hence the single-parameter scaling is unable to describe the transition.

(3) We find that the conductances show strong nonmonotonic variations with  $L$  and a subtle structure of resonant peaks and subpeaks. In one dimension, we find that (a) the positions of these peaks can be related to the properties of the irrational number that characterizes the quasiperiodicity of the potential and (b) the  $L$  dependence of the Thouless conductance is multifractal.

(4) We show clearly that the Thouless and Landauer conductances are not the same in quasiperiodic systems, in contrast to what is observed in random systems.

(5) We find that, as  $d$  increases, this nonmonotonic dependence of  $g$  on  $L$  weakens and, in three dimensions, our results for  $\beta(g)$  are reasonably well described by single-parameter scaling.

Thus our results demonstrate that there is a complete violation of single-parameter-scaling theory at the metal-insulator transition in one- and two-dimensional quasiperiodic systems, but a remarkable (approximate) restoration of this theory in three-dimensional quasiperiodic systems.

The remainder of this paper is organized as follows. In Sec. II we describe the models we study and give an overview of our main results. Section III is devoted to the description of our results for Thouless and Landauer conductances and  $\beta$  function. In Sec. IV we discuss the implications and significance of our results.

## II. MODEL AND OVERVIEW OF RESULTS

We study the scaling of the conductance  $g$  with the system size  $L$  across the localization-delocalization (insulator-metal) transition in the well-known 1D quasiperiodic Aubry-Andre Hamiltonian [3],

$$\mathcal{H} = \sum_r (e^{i\phi} c_r^\dagger c_{r+1} + \text{H.c.}) + 2V \sum_r \cos(2\pi br + \phi) c_r^\dagger c_r, \quad (1)$$

and its  $d$ -dimensional generalizations [27] (see Appendix A). We set to unity the nearest-neighbor hopping amplitude of electrons, which are created by  $c_r^\dagger$  on the site  $r$ , and we characterize the on-site quasiperiodic potential by its strength  $V$  and an irrational number  $b$ , which we choose to be a quadratic irrational, e.g., the golden ratio conjugate  $b = \Phi = (\sqrt{5} - 1)/2$ . The phase  $\phi \in [0, 2\pi)$  induces a shift of the potential, so we use it to generate a statistical ensemble for a fixed  $b$ . This model (1) and its generalizations to two and three dimensions (Appendix A) are all self-dual at  $V = 1$ . In one dimension, this self-dual point coincides with the delocalization-localization transition between a localized insulator ( $V > 1$ ) and a ballistic metal ( $V < 1$ ) [3]; by contrast, in three dimensions, the self-dual point lies within a diffusive-metal phase, which separates localized and ballistic phases. These two phases are connected by a real- and momentum-space duality, akin to that in the 1D model [27]; so, in three dimensions, we expect the localized-to-diffusive metal and ballistic-to-diffusive metal transitions to be dual to each other [27]. We carry out detailed studies of electrical transport in all these phases and across the transitions between them in the 1D Aubry-Andre model and its generalizations to two and three dimensions. We summarize our principal results below.

We compute the Thouless,  $g_T(E, L)$ , and Landauer,  $g_L(E, L)$ , conductances, at a given energy  $E$ , for a hypercube of volume  $L^d$  ( $d = 1, 2$ , and  $3$ ), as a function of the length  $L$  and at zero temperature; we obtain the averages of these conductances by varying  $\phi$ . We find that *even* the typical conductances,  $g(L)$  (either  $g = g_T$  or  $g_L$ ) are *strongly* nonmonotonic functions of  $L$ ; this implies that a strict application of single-parameter-scaling theory is untenable, especially in one and two dimensions. This nonmonotonicity is present in three dimensions too, but it is weaker than in two and one dimensions. The average  $L$  dependence of these conductances, in one and two dimensions, for the localized, critical, and delocalized states, can be characterized by average, *smooth* curves [denoted generically by  $\tilde{g}(L)$ ]; from these smooth curves we can obtain the associated  $\beta$  functions [ $\beta(\tilde{g})$ ] for large system sizes.

In one dimension, these  $\beta$  functions show discontinuous jumps as we go from localized [ $\beta(\tilde{g}) \sim \ln(\tilde{g})$ ] to ballistic metallic states across the transition at  $V = V_c = 1$ ; the critical state exhibits subdiffusive power-law scaling,  $\tilde{g} \sim L^\alpha$ , such

that  $\beta(\bar{g}) = \alpha < d - 2 = -1$ . This subdiffusive scaling is less clear in two dimensions than in one dimension because the onset of the scaling regime occurs only above a large, microscopic length scale  $\ell$ ; nevertheless, our calculation of the open-system conductance in two dimensions suggests a similar jump in the  $\beta$  function via a subdiffusive critical state at  $V_c = 1$ . Furthermore, instead of ballistic scaling for the conductance in the metallic phase, we find superdiffusive behavior, with a constant  $\beta(\bar{g})$  that lies between  $d - 2$  and  $d - 1$ .

Our results in three dimensions are consistent with a continuous metal-insulator transition at  $V_c \simeq 2.2$ . We obtain scaling collapse for  $g_L(L)$  near the transition, with a correlation-length exponent  $\nu \simeq 1.6$ , a value that is close to the value of this exponent for the Anderson-localization transition in three dimensions (as found in the recent study of Ref. [27], which used moments of the wave function). Moreover, we obtain a continuous  $\beta$  function from this scaling collapse; this suggests that the single-parameter-scaling theory is a reasonably good approximation for the 3D quasiperiodic system we consider. However, a weak, nonmonotonic  $L$  dependence of the conductance remains and indicates deviations from strict, single-parameter scaling. We do not find a sharp transport signature of the diffusive-metal-to-ballistic transition at  $V \simeq 1/V_c$ , which we expect from duality [27]. Given the system sizes we have been able to use in our study in three dimensions, we find that the metallic phase, for  $V \lesssim 1/V_c$ , exhibits superdiffusive scaling for  $\tilde{g}_L(L)$ , with a  $V$ -dependent exponent  $1 < \alpha < 2$  that approaches the ballistic limit ( $\alpha = 2$ ) asymptotically for  $V \rightarrow 0$ .

The nonmonotonic variation of the conductance with  $L$  is most prominent in one dimensions, especially for  $g_T(L)$ , which exhibits resonant transport peaks for sequences of  $L$  that depend on the particular quadratic irrational number we use; e.g., for  $b = \Phi$ , different sequences of peaks occur at the Hemachandra-Fibonacci numbers and their combinations. At the critical point, each one of these sequences exhibits power-law scaling, i.e.,  $g_T(L) \sim L^\alpha$  with the exponent  $\alpha$  ranging from the almost-diffusive ( $\alpha \simeq -1$ ) to the subdiffusive ( $\alpha < -1$ ) values for different sequences. We carry out a fractal analysis [30] of the  $g_T$  vs  $L$  plot to obtain multifractal scaling; we quantify this multifractality of the nonmonotonic variations of  $g_T$  with  $L$  via the singularity spectrum  $f(\alpha)$  [30]. (We use the standard notation  $\alpha$  for the crowding index [31]; this should not be confused with the exponent  $\alpha$  for the power-law scaling of the conductances). At the critical point, we find a broad singularity spectrum  $f(\alpha)$ ; this narrows in the metallic phase. Such multifractal scaling of the conductances, as a function of  $L$ , is a fundamental difference between quasiperiodic and random systems. Our multifractal analysis shows clearly that the conventional assumption about the conductance scaling as a simple power of  $L$  is invalid here.

We show that  $g_L(L)$  also fluctuates with  $L$ ; however, it does not exhibit prominent resonant peaks at distinct sequences of lengths, even in one dimension. Hence, our results indicate a clear distinction between isolated and open-system conductances, as measured through Thouless and Landauer conductances, respectively. Our results reveal very rich transport properties for finite-size quasiperiodic systems; especially in

one and two dimensions, these properties are significantly different from their counterparts for random systems.

In the next section we discuss our results in detail. We give some additional aspects of our calculations and numerical computations in the Supplemental Material [32].

### III. RESULTS

#### A. Thouless conductance

We first characterize the response of our isolated, finite system to boundary perturbation through the Thouless conductance,  $g_T = \delta E / \Delta_E$ , where  $\delta E$  is the shift of the energy levels, around energy  $E$ , when we change the boundary conditions from periodic,  $\psi(r_\mu + L) = \psi(r_\mu)$ , to antiperiodic,  $\psi(r_\mu + L) = -\psi(r_\mu)$  [33,34], in a particular direction  $\mu = 1, \dots, d$ ;  $\Delta_E$  is the level spacing at energy  $E$ . In a diffusive metal,  $g_T$  can be argued to be the same as the usual Landauer  $g_L$  [33–35] and, in the insulating state, it is expected that  $\ln(g_L) \propto \ln(g_T)$  [36]. However, it should be noted that  $g_T$  is a property of a closed, finite system with discrete energy eigenvalues; by contrast, in the usual transport setup, the system is connected to infinite leads and hence it has a continuous spectrum. As we show below for the quasiperiodic system we consider, this makes  $g_T(L)$  significantly different from  $g_L(L)$ .

We note that there is always some ambiguity in the definition of  $g_T$  [33], e.g., whether we should use the geometric or the arithmetic mean for  $\delta E$  and  $\Delta_E$ . We employ the geometric mean to estimate  $\delta E$ . For most of our results, we use the arithmetic mean for the energy-level spacing  $\Delta_E$ , around  $E$ , to obtain  $g_T$ . We have also calculated the Thouless conductance  $g_T^{\text{typ}}$ , by using the typical level spacing  $\Delta_E^{\text{typ}}$ , obtained from the geometric mean (see the Supplemental Material [32], Sec. S1 1). As discussed below, we find most of the qualitative features of  $g_T$  and  $g_T^{\text{typ}}$  to be same; e.g., both decay exponentially with  $L$  in the insulating phase, show the hierarchical structure of peaks, and multifractal scaling. At the critical point in one dimension,  $g_T^{\text{typ}}$ , and not of  $g_T$ , compares better with the Landauer conductance  $g_L(L)$ , in terms of the overall scaling with  $L$ . However,  $g_T^{\text{typ}}$  shows *unphysical* superballistic behavior in the metallic side in one dimension:  $g_T^{\text{typ}}$  increases with increasing  $L$ , in contrast to ballistic scaling of  $g_L(L)$ . Hence, we discuss, principally, our results for  $g_T$ , which we obtain by using the mean level spacing  $\Delta_E$ .

We obtain the mean  $\langle g_T \rangle(E, L)$  or typical conductance  $\exp[\langle \ln g_T(E, L) \rangle]$  at an energy  $E$  by computing single-particle energy eigenvalues, for both periodic and antiperiodic boundary conditions, via numerical diagonalization of the Hamiltonian in Eq. (1) or its  $d$ -dimensional generalizations [Eq. (A1), see the Methods section], without the phase factor  $\phi$  in the hopping term. The typical and mean Thouless conductances give similar results in one dimension. The latter,  $g_T$  at  $E = 0$ , is plotted versus  $L$  for  $b = \Phi$  in Fig. 1, for insulating and metallic phases [Fig. 1(a)] and also at the critical point  $V = 1$  [Fig. 1(b)]. We find strong nonmonotonicity of  $g_T(L)$ . We first characterize its overall  $L$  dependence by a smooth least-square-fitting curve  $\tilde{g}_T(L)$ , which shows ballistic behavior in the metallic phase, i.e.,  $\tilde{g}_T$  independent of  $L$ ; in contrast, the conductance in the localized phase is well described by  $\tilde{g}_T(L) \simeq g_0(V)e^{-L/\xi}$  even very close to the transition,  $V \gtrsim V_c$ ;

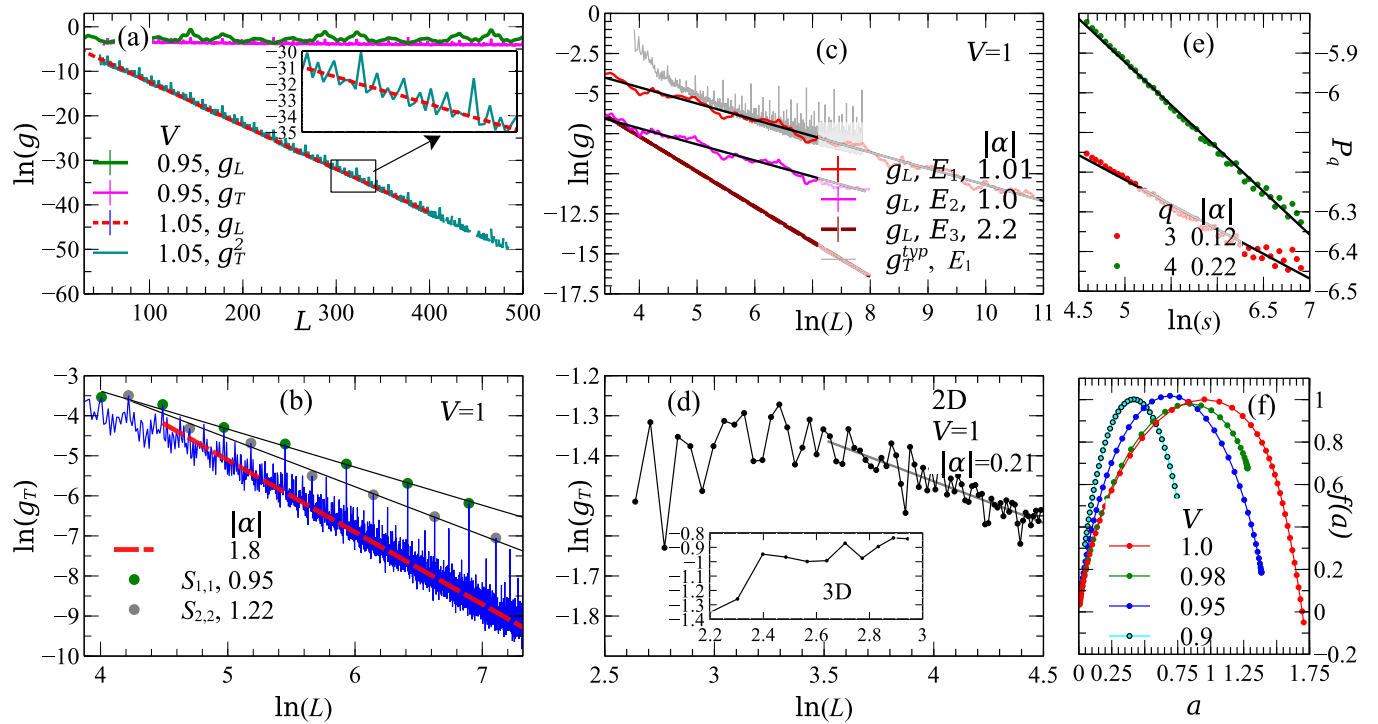


FIG. 1. Length-dependent conductances and multifractality in the Aubry-Andre model in one dimension and its 2D and 3D generalizations. (a) Semilog plots vs  $L$  of the conductances  $g_T$  (Thouless) and  $g_L$  (Landauer) at illustrative values of  $V$  in the metallic ( $V = 0.95$ ) and insulating ( $V = 1.05$ ) regimes in one dimension. On the metallic side, both  $g_T$  and  $g_L$  show *nonmonotonic* (roughly speaking, small-wavelength) fluctuations about an  $L$ -independent mean value. On the insulating side,  $g_T^2 \propto g_L$ ; both  $g_L$  and  $g_T$  decay exponentially with  $L$ , the latter only on average because  $g_T$  still displays *nonmonotonic* fluctuations (enlarged view in the inset). (b) Log-log plots vs  $L$  of the Thouless conductance  $g_T$ , at the  $1d$  critical point  $V = 1$ , showing an average decay (dashed red line) with  $g_T \propto L^\alpha$  and  $\alpha \simeq -1.8$ , with hierarchically organized peaks, whose heights also decay as a power of  $L$  but with different exponents (for notational simplicity denoted generically by  $\alpha$ ), which depend on  $\mathcal{S}_{L_1, L_2}$ , the set of peaks at the lengths  $L_{i+1} = L_i + L_{i-1}$ , with the seed lengths  $L_1$  and  $L_2$ ; for the illustrative sets  $\mathcal{S}_{1,1}$  (green filled circles) and  $\mathcal{S}_{2,2}$  (blue filled circles) we obtain the decay exponents  $\simeq -0.95$  and  $\simeq -1.22$ , respectively. (c) Log-log plots vs  $L$  of the Landauer conductance  $g_L$ , at the  $1D$  critical point  $V = 1$ , showing an average decay  $g_L \propto L^{\alpha(E)}$ , with energy-dependent exponents  $\alpha(E)$ , shown for the representative energies  $E_1 = 0$  [ $\alpha(E_1) \simeq -1.01$ ],  $E_2 = 1.98496$  [ $\alpha(E_2) \simeq -1.0$ ], and  $E_3 = 0.18906032$  [ $\alpha(E_3) \simeq -2.2$ ; see text]; note the nonmonotonic fluctuations about these mean-decay lines. The grey curve shows the Thouless conductance ( $g_T^{\text{typ}}$ ) obtained by using the typical level spacing (see text) at  $E_1 = 0$ ; its overall slope is close to that of the  $g_L$ ;  $g_T^{\text{typ}}$  has been scaled to fall on top of  $g_L$ . (d) This nonmonotonicity in log-log plots of  $g_T(L)$  vs  $L$  persists in two and three dimensions (inset), as we show by illustrative data at the metal-insulator critical points; in two dimensions, the critical  $g_T(L) \sim L^{-0.21}$  exhibits an overall subdiffusive scaling. (e) A fractal analysis of the  $L$  dependence of the energy-averaged  $g_T$ , i.e.,  $g_T^\infty$  (see the Supplemental Material [32] Sec. S1 2 and the main text) reveals multifractal scaling of the nonmonotonic variations of  $g_T(L)$  at the critical point. (f) A plot of the singularity spectrum  $f(\alpha)$  vs  $\alpha$  corroborates this multifractality (see main text); note that the singularity spectrum narrows on the metallic side  $V < 1$ .

$g_0$  denotes conductance at a microscopic length scale  $\ell \approx 1$  and it depends on  $V$ . However, the critical state exhibits an overall power-law dependence on  $L$ ,  $\tilde{g}_T \sim L^\alpha$  [the dashed red line in Fig. 1(b)] with  $\alpha \simeq -1.8$ , up to the maximum system size we have studied ( $L = 3000$ ).

The nonmonotonicity of the Thouless conductance is clearly manifested in the peak and subpeak structure of  $g_T(L)$ , in both the metallic and insulating phases [Fig. 1(a)]. These peaks are most striking at the critical point [Fig. 1(b)], where we find hierarchically organized peaks, whose heights decay as a power of  $L$  but with different exponents (for notational simplicity denoted generically by  $\alpha$ ), which depend on  $\mathcal{S}_{L_1, L_2}$ , the set of peaks at the lengths  $L_{i+1} = L_i + L_{i-1}$ , with the seed lengths  $L_1$  and  $L_2$ ; for the illustrative sets  $\mathcal{S}_{1,1}$  (green filled circles and  $L_i = F_i$ , the Fibonacci numbers) and  $\mathcal{S}_{2,2}$  (blue filled circles and  $L_i = 2F_i$ ) we obtain the decay exponents

$\simeq -0.95$  and  $\simeq -1.22$ , respectively. We can also identify similar sequences of peaks in the metallic and insulating phases [Fig. 1(a)]. The development of a quantitative theory of these peaks and their decay exponents  $\alpha_S$  is an important challenge. At the critical point  $g_T^{\text{typ}}$  shows the same qualitative behavior as  $g_T(L)$ , in terms of the peak structure related with  $\mathcal{S}_{L_1, L_2}$ ; but the former scales with a different overall exponent, which is much closer to that of the open system conductance as shown in Fig. 1(c).

Similar resonance peaks have been seen at high- or infinite-temperature open-system transport [13–15]; however, this resonance effect is much more striking in the  $g_T$  that we calculate. We find similar resonant peaks for the energy-averaged or infinite-temperature Thouless conductance  $g_T^\infty$  as well (see the Supplemental Material [32]). The existence of sharp resonant peaks in  $g_T(L)$ , up to arbitrarily large lengths,

is a special feature of one dimension and points to markedly distinct transport characteristic of the quasiperiodic system compared to random systems in one dimension. We find the resonant peaks to be present in two and three dimensions, albeit much less prominently than in one dimension, as we show in Fig. 1(d) at the metal-insulator transition  $V = V_c$ .

### Conductance multifractality

We next ask whether the strong, nonmonotonic variations of  $g_T$  with  $L$  in one dimension [Figs. 1(a) and 1(b)] can be quantified by fractal analysis methods. Motivated by the multiple power laws in Fig. 1(b) for different sequences of  $L$ , we carry out a fluctuation analysis [30] of  $g_T$ , as function of  $L$ , by using methods that are used to treat fractal time series (see the Supplemental Material [32]). We find the intriguing result that  $g_T(L)$  exhibits multifractal scaling of different moments, as we show for a few moments in Fig. 1(e). We also calculate the singularity spectrum [30,31,37] of  $g_T(L)$  (see the Supplemental Material [32]). As we show in Fig. 1(f), this singularity spectrum  $f(\alpha)$  indicates substantial multifractality at the critical point; it narrows in the metallic phase, but multifractality still persists there. A meaningful multifractal analysis cannot be performed in the insulating phase because the values of the conductance become exponentially small with  $L$ . We have verified that the same kind of multifractality is also present in  $g_T^{\text{typ}}(L)$ . We emphasize that the multifractality of conductance reported here is distinct from the usual multifractality of wave functions or two-point conductances [19] at the 3D Anderson transition for random systems. In the latter, typical and mean conductances are monotonic functions of  $L$ , and, as a result, the particular multifractality of  $g_T(L)$ , which we find here for the 1D quasiperiodic system, would be absent. To this end, we show in the Supplemental Material [32] that the usual multifractality of the critical wave function, as measured in the 3D Anderson transition [19], is also present for quasiperiodic systems in one dimension [38–41].

We have not been able to carry out a detailed multifractal analysis of  $g_T(L)$  in  $d = 2, 3$  because of the limitations of the system sizes in the calculation of the Thouless conductance which requires the numerical diagonalization of large matrices. Moreover, the scales of the nonmonotonic variations are much weaker in two and three dimensions, compared to those in one dimension, as is evident from Figs. 1(b) and 1(d).

### B. Open-system conductance

We next study the conductance of open systems, starting with Aubry-Andre chain connected to two semi-infinite leads at both ends. In this case, we compute the Landauer or Economou-Soukoulis conductance  $g_L(E) = T(E)$  [42,43], where

$$T(E) = 4 \sin^2 k / |e^{-ik} \psi(L) - \psi(L-1)|^2$$

is the transmission coefficient at energy  $E = 2t \cos k$ ,  $t$  being the hopping amplitude in the tight-binding leads, and where the wave-function amplitudes  $\psi(L)$ ,  $\psi(L-1)$  are obtained by using a standard transfer-matrix method (see the Supplemental Material [32]). For dimensions  $d = 2, 3$ , we calculate the open-system conductance  $g_K$  by using the Kubo formula for the system connected with leads and the recursive

Green-function method [23,25] (see the Supplemental Material [32]). The open-system Kubo conductance gives results identical to those for the Landauer conductance [44], as we have verified for one dimension by calculating both  $g_L$  and  $g_K$ .

#### 1. One dimension

Our results for  $\phi$ -averaged typical conductance  $\exp(\ln g_L(E=0, L))$ , denoted by  $g_L$  for brevity, are plotted in Figs. 1(a) and 1(c) across metal-insulator transition in one dimension. The overall length dependence in the metallic and insulating phases are the same as that of  $g_T(L)$ , namely, ballistic and localized behaviors with  $L$ , respectively. The transport at the critical point is almost diffusive, with  $g_L \sim L^{-1.01}$  for  $E = 0$ , similar to that obtained from the overall  $L$  dependence of  $g_T^{\text{typ}}$ . Because the 1D Aubry-Andre chain has a fractal energy spectra dominated by gaps [4,7–10], it is hard to track the  $L$  dependence for an arbitrary energy, as it can move into a gap as  $L$  is varied. As a result,  $g_L(E)$  can cease to show the power-law scaling and instead exhibits an exponential decay with  $L$ . However, we have been able to track the nearly diffusive power law up until the largest system size we have used ( $L = 5 \times 10^4$ ) studied for  $E = 0$  and also for a few other values of  $E$ , different power laws are observed till sufficiently large  $L$  as shown in Fig. 1(c). This conductance, at one of the energies ( $E \simeq 0.189$ ), shows strongly subdiffusive behavior with  $\alpha \simeq -2.22$ . Because conductances at different energies show a range of scaling, from diffusive to subdiffusive, it is possible to obtain an overall subdiffusive conductance scaling at high temperature that averages over a large energy window, as in earlier studies [13–15]. To summarize, both  $g_L$  and  $g_T$  indicate the presence of multiple power-law exponents that depend on the energy and/or the sequence  $S$ .

As is evident from Figs. 1(a) and 1(c) [see also Figs. S3 (a)–(d), Supplemental Material [32]], the Landauer conductance in one dimension also shows strong nonmonotonic dependence on  $L$ , both in the metallic and critical states, even after averaging over sufficiently large numbers of  $\phi$ 's (see the Methods section) and there are peaks and subpeaks as in  $g_T$ , e.g., the dominant peaks appear at some of the Fibonacci numbers. However, peaks are much weaker and do not appear at all  $F_n$ 's. The weakening, and the absence in some cases, of the conductance peaks in open-system conductance, as opposed to that in  $g_T$ , indicate that the leads affect conductances significantly by broadening and even washing out the resonances.

#### 2. Two dimensions

The open-system Kubo conductance  $g_K(L)$  for  $E = 0$  in two dimensions is shown in Fig. 2(a). Our results for system sizes up to  $1000^2$  are consistent with a metal-insulator transition at  $V = V_c = 1$ , the self-dual point. The conductance in the localized phase, as in one dimension, follows  $g_K(L) \simeq g_0(V) \exp(-L/\xi)$  for  $V > V_c$ . The metallic phase for  $V < V_c$  is superdiffusive, with  $g_K(L) \sim L^\alpha$  and  $d - 2 < \alpha \simeq 0.35 < d - 1$ , lying between diffusive and ballistic limits. Here,  $g_0(V)$  is the conductance at a microscopic length scale  $\ell$ . We find the asymptotic scaling behaviors set in only for  $L \gg \ell$ , where the microscopic length  $\ell(V)$  is substantially

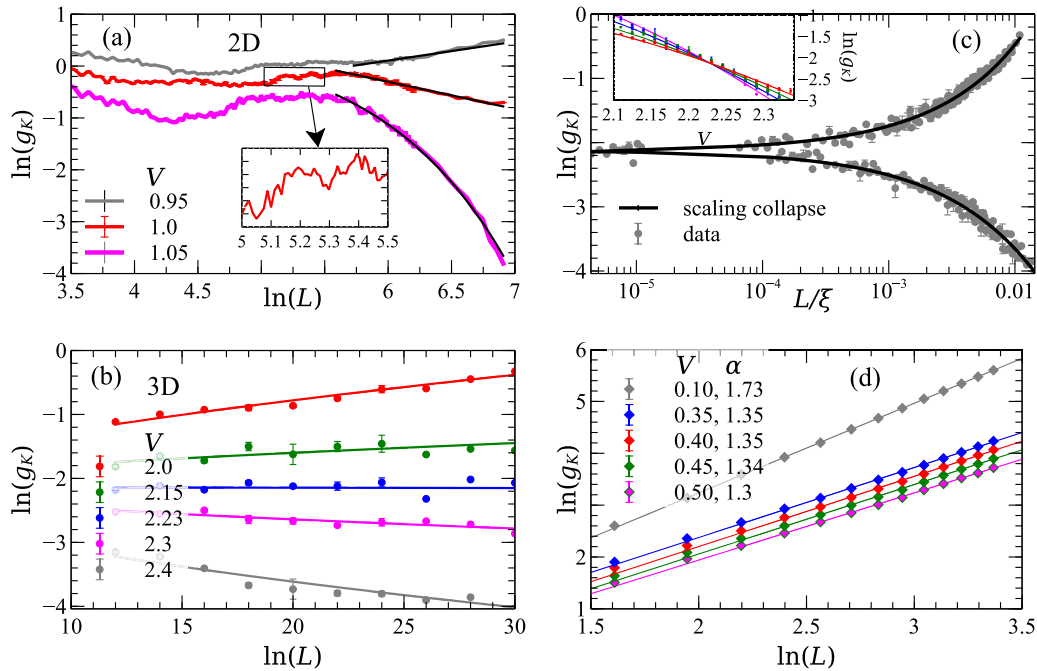


FIG. 2. Open-system conductance in two and three dimensions. (a)  $g_K(E = 0, L)$  for insulating ( $V = 1.05$ ), critical ( $V = 1$ ), and metallic ( $V = 1$ ) states in two dimensions. The solid black lines are fits of the data for the asymptotic  $L$  dependence, exponential decay for the insulating state and power-law scalings for critical and metallic states. The nonmonotonicity of  $g_K(L)$  is shown in the inset. (b)  $g_K(L)$  across localized to diffusive metal transition in three dimensions. A weak nonmonotonic variations, larger than the error bars, can be seen. The solid lines are fit to the data obtained via scaling collapse, shown in (c). The inset in (c) clearly indicates the critical point at  $V_c = 2.22 \pm 0.01$  in terms of a crossing of  $g_K$  vs  $V$  curves for different  $L$ . (d) Conductance near  $V = 1/V_c \simeq 0.45$  follows superdiffusive scaling,  $g_K \sim L^\alpha$  with  $1 < \alpha < 2$ , as shown by the fits (solid lines) to the data points and it asymptotically approaches to the ballistic scaling deep in the metallic side, e.g.,  $\alpha = 1.73$  for  $V = 0.1$  as shown.

large, varying between  $L = 50$  and  $500$  depending on  $V$ . Irrespective of  $V$ ,  $g_K(L)$  shows an initial ballistic increase [not shown in Fig. 2(a)], followed by an intermediate regime of length, only after which the scaling regimes ensue. The critical point at  $V = V_c$  exhibits a subdiffusive length scaling of the conductance with  $\alpha \simeq -0.52$ . Again, strong nonmonotonic variations of  $g_K(L)$  are observed in all the phases, as demonstrated, e.g., in the inset of Fig. 2(a) for the critical state.

### 3. Three dimensions

Our results for the 3D conductances  $g_K(L)$  are shown in Fig. 2(b) up to  $L = 30$  near  $V = 2.2$ . As evident, non-monotonic variations of  $g_K(L)$ , though present, are drastically reduced for three dimensions, in contrast to those in one and two dimensions [Figs. 1(a), 1(c) and 2(a)]. A critical point at  $V = V_c \simeq 2.2$  can be clearly detected from the crossing of curves as function of  $V$  for different system sizes, as shown in the inset of Fig. 2(c). The crossing also indicates a scale invariant conductance at the critical point. A reasonably good scaling collapse of the data using a single-parameter finite-size scaling form  $\ln[g_K(L)] = \mathcal{F}[(V_c - V)L^{1/\nu}]$  could be obtained near the critical point, as shown in Fig. 2(c). The finite-size scaling yields  $\nu = 1.60 \pm 0.04$  and  $V_c = 2.22 \pm 0.01$ , consistent with earlier study in Ref. [27] using multifractal finite-size scaling analysis of wave function of closed system. The universal scaling curve describes the  $g_K(L, V)$  data quite

well as shown by the solid lines in Figs. 2(b) and 2(c) (inset). This is in tune with a continuous  $\beta(g)$  and single-parameter scaling law,  $\beta(g) = d \ln g / d \ln L$ , at the metal-insulator transition in the 3D quasiperiodic system, unlike those in the 1D and 2D quasiperiodic systems. However, the persistence of weak nonmonotonic system-size variations in the typical conductance still violates the assumption of monotonicity of  $\beta(g)$  in the scaling theory [1]. The weak nonmonotonicity, though, could be due to limited system sizes accessed in three dimensions and one might recover strict single-parameter scaling at larger lengths.

From the real-space-momentum space duality of the model [(A1)], we expect another transition around  $V \sim 1/V_c \approx 0.45$  from a diffusive to a ballistic phase [27]. Our results do not show any transport signature of this transition. As shown in Fig. 2(d),  $g_K(L)$  around  $V = 0.45$  can be well described by superdiffusive length scaling with an exponent  $\alpha > 1$ . This could be due to the fact that the duality is not strictly valid for such a finite system connected to leads and due to the dichotomy between open and closed system properties, as seen in the 1D quasiperiodic system [13,14].

### C. $\beta$ function

As we have remarked already, the strong nonmonotonicity of even the typical  $g(L)$ , in one and two dimensions, invalidates the application of single-parameter scaling. However,

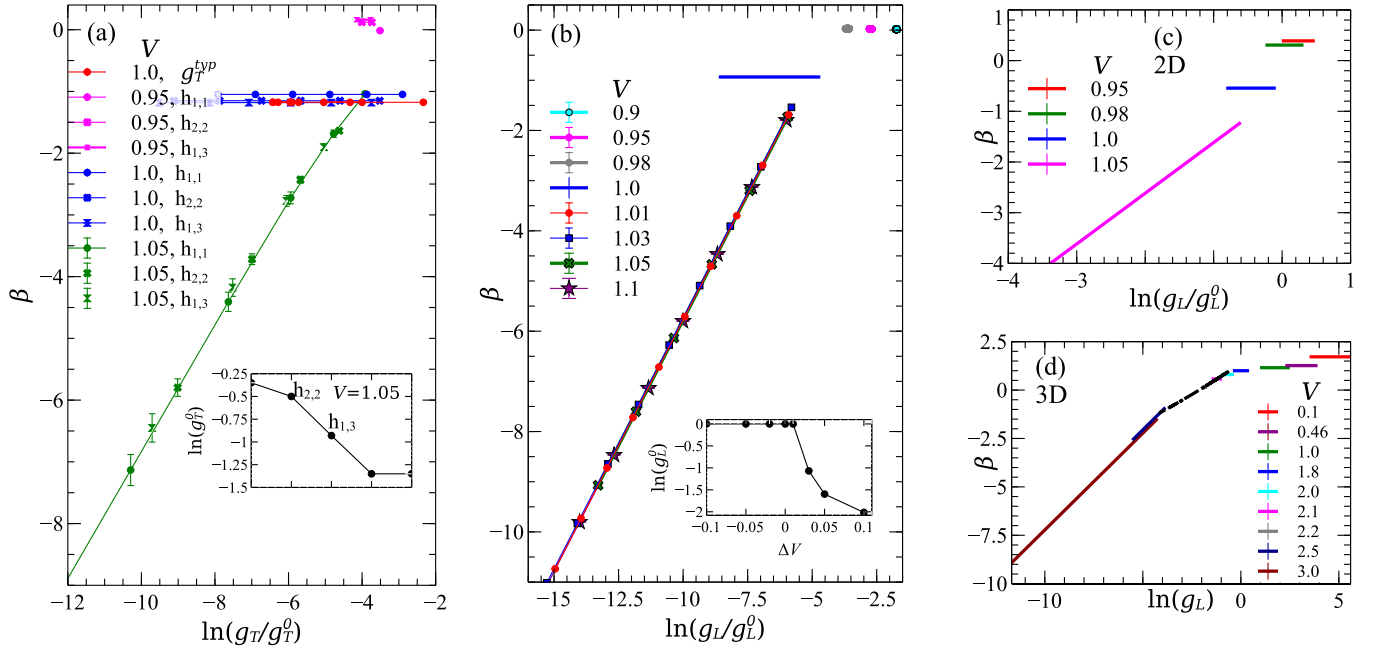


FIG. 3.  $\beta$  functions in one, two, and three dimensions. (a)  $\beta(\tilde{g})$  in one dimension extracted from  $\tilde{g}_T$  across metal-insulator transition for various sequences  $\mathcal{S}_{L_1, L_2}$ , obtained by fitting with exponential decay and power law for  $V > 1$  and  $V \leq 1$ , respectively. Same color with different symbols represents  $\beta(\tilde{g}_T)$  calculated for different  $\mathcal{S}$  and the same  $V$ . The red curve at the critical point corresponds to the  $\beta$  function extracted from the overall behavior of  $g_T^{\text{yp}}(L)$ . On the insulating side to make all the curves fall on the same line we choose different microscopic conductance ( $g_T^0$ ) for different sequence (inset).  $\beta(\tilde{g})$  extracted in similar manner for (b)  $\tilde{g}_L$  in one dimension, (c)  $\tilde{g}_K$  in two dimensions, and (d)  $\tilde{g}_K$  in three dimensions (solid lines) for values of  $V$  indicated in the figure panels. In (b) and (c) the straight lines for  $\beta(\tilde{g}_L)$  in the insulating side ( $V > 1$ ) have been collapsed to a single curve by choosing an appropriate  $g_L^0(V)$ , as shown for one dimension in the inset of (b). In (d) the black dashed line is the  $\beta$  function calculated from the scaling collapse of Fig. 2(b).

we construct a  $\beta(\tilde{g})$ , where  $\tilde{g}(L)$  is extracted from fitting a smooth curve to our data for  $g_T(L)$  and  $g_L(L)$ , e.g., the ones shown for several values of  $V$  in Figs. 3(a) and 3(b). This is an unambiguous procedure in one dimension, where the overall  $L$  dependencies of the conductances in the localized, critical, and metallic states are very well described by exponentially localized, subdiffusive, and ballistic behaviors, respectively, over several decades of  $L$  [Figs. 1(a) and 1(c)]. The results for the respective  $\beta$  functions  $\beta(\tilde{g})$  in one dimension are shown in Figs. 3(a) and 3(b) across the metal-insulator transition. In Fig. 3(a),  $\beta(\tilde{g}_T)$  has separate curves for individual phases and the critical point, as well as for different sequences. For example, the multiple straight lines at the critical value  $V = 1$  arise because of distinct power laws for different sequences shown in Fig. 1(b). These, and the jump of  $\beta$  functions across the critical point, clearly violate the assumption of continuity in the single-parameter-scaling theory. Similar features are seen in  $\beta(\tilde{g}_L)$  [Fig. 3(b)]. We find that  $\tilde{g}_L(V, L) = g_0(V) \exp[-L/\xi(V)]$  describes quite accurately the conductance in the localized phase, even very close to the transition. However, the coefficient  $g_0$ , a measure of conductance at the microscopic scale  $\ell$ , varies substantially with  $V$  [see inset of Fig. 3(b)]. This is unlike, e.g., that in the 1D Anderson model where  $g_0 \approx 1$  irrespective of the disorder strength. As a result, we can only obtain a universal  $\beta(\tilde{g})$  curve for the localized phase in one dimension as a function of  $\ln[\tilde{g}_L/g_0(V)]$ , i.e., after dividing  $g_L$  with the appropriate  $g_0$ .

To contrast the above results for the  $\beta$  function for our 1D quasiperiodic system with that of a random system, we show, in the Supplemental Material [32], that even a small amount of randomness, introduced, e.g., by elevating the phase  $\phi$  to a random variable at each site, makes  $g_L(L)$  decay exponentially with  $L$ , but with small nonmonotonicity, and hence leads to a continuous  $\beta$  function for the overall conductance.

We also note that the violation of single-parameter finite-size scaling and the multifractality of the typical Thouless conductance (Sec. III A), which we find in 1D transport, are distinct from the nonpower law criticality and multifractality of the energy spectrum found in a recent work [45] on quasiperiodic potentials characterized by irrational numbers without a periodic-continued-fraction representation. This is unlike that in our model with  $b = (\sqrt{5} - 1)/2$ , which can be represented by a periodic continued fraction.

As shown in Fig. 3(c), we find a very similar result for  $\beta(\tilde{g})$  in two dimensions, which we extract from the fitting curves in Fig. 2(a). Here the  $\beta$  function also jumps from a localized behavior,  $\beta(\tilde{g}) \propto \ln(\tilde{g}/g_0)$ , to a constant superdiffusive value  $\beta(\tilde{g}) \simeq 0.3$  in the metallic phase, across a subdiffusive critical state with  $\beta(\tilde{g}) \simeq -0.52$ . However, as we have commented earlier, the asymptotic scaling behaviors in two dimensions can only be extracted for  $L$  above a substantially large microscopic length scale  $\ell$  and hence the  $\beta$  functions are extracted from only a limited ranges of system sizes.

Our results in both one and two dimensions indicate a strong violation of the assumption of continuity of  $\beta(g)$  in

the single-parameter-scaling theory, even when we disregard the nonmonotonicity of  $g(L)$ , by extracting an overall, smooth  $\tilde{g}(L)$  from the asymptotic behaviors at  $L$ . The above procedure cannot be carried out in three dimensions, close to the critical point, because our system sizes are limited to much smaller values of  $L \leq 30$ . However, given that the nonmonotonicity of  $g(L)$  is much weaker in three dimensions, we can obtain a reasonable scaling collapse of our data near the metal-insulator transition. We extract  $\beta(g)$  in Fig. 3(d) (dashed black line) near the transition from the scaling fit of  $g_K(L)$ , shown in Figs. 2(b) and 2(c). The fit describes the data well over a reasonably large range of  $V$  and  $L$  and hence suggests the restoration of continuity of  $\beta(g)$  for the 3D quasiperiodic system, provided we neglect the weak nonmonotonic variations of  $g(L)$ . In Fig. 3(d), we also show that the  $\beta$  function, extracted from exponential fits deep in the insulating phase and from power-law fits deep in the metallic phase, is consistent with that obtained from the scaling collapse near the transition.

#### IV. CONCLUSIONS

In summary, we have studied transport properties in a particular class of self-dual quasiperiodic models in one, two, and three dimensions. We have focussed on the system-size dependencies of the Thouless and open-system Landauer/Kubo conductances. Our results uncover the intricate nature of transport in quasiperiodic systems, which is manifested in the nonmonotonic system-size dependence of typical conductances, e.g., because of transport resonances, and a variety of subdiffusive power laws for critical transport; these depend on the dimension, energy, and the sequences of length we have described above.

Our results reveal the absence of a single-parameter-scaling description in low dimensions and an approximate recovery of single-parameter scaling in three dimensions; this has direct implications for universality classes of metal-insulator transition in quasiperiodic systems. In ongoing work we are computing the multifractal spectrum of the wave function and the Thouless conductance at the critical point in the 3D quasiperiodic model and comparing it with those at the 3D Anderson transition to verify whether they truly belong to the same universality class. It is also worthwhile to look into generalizations of quasiperiodic systems to other symmetry classes [27] from this perspective. Moreover, it would also be interesting to study the implications of subdiffusive critical states of noninteracting models, specially in one dimension, on the Griffith-like effect seen experimentally near the MBL transition in the interacting quasiperiodic system [46] and to incorporate these critical states into a real-space renormalization-group framework [47–49] for the MBL transition in quasiperiodic systems.

#### ACKNOWLEDGMENTS

We thank S. Ganeshan, S. Sondhi, A. Purakayastha, and C. Dasgupta for useful discussions. S.B. acknowledges support from The Infosys Foundation, India. S.M. acknowledges support from the Indo-Israeli ISF-UGC grant. We acknowledge support from DST, UGC, and CSIR (India).

#### APPENDIX: $d$ -DIMENSIONAL GENERALIZATION OF AUBRY-ANDRE MODEL

We study the model proposed in Ref. [27] as a generalization of the self-dual 1D Aubry-Andre model to  $d$  dimensions, namely,

$$\mathcal{H} = t \sum_{\mathbf{r}, \mu} (e^{i\phi_\mu} c_{\mathbf{r}+\hat{\mu}}^\dagger c_{\mathbf{r}} + \text{H.c.}) + \sum_{\mathbf{r}} \epsilon_{\mathbf{r}} c_{\mathbf{r}}^\dagger c_{\mathbf{r}}, \quad (\text{A1a})$$

$$\epsilon_{\mathbf{r}} = 2V \sum_{\mu=1}^d \cos \left( 2\pi \sum_{\nu=1}^d B_{\mu\nu} r_\nu + \phi_\mu \right), \quad (\text{A1b})$$

where  $c_{\mathbf{r}}$  is the fermion operator at site  $\mathbf{r}$  of a  $d$ -dimensional hypercubic lattice and  $\mu = 1, \dots, d$  denotes Cartesian components. We choose  $t = 1$ , the matrix  $\mathbb{B} = b\mathbb{R}$ , with  $b = \Phi$ , and an orthonormal matrix  $\mathbb{R}$  [27]. In one dimension,  $\mathbb{R} = 1$ , and

$$\mathbb{R} = \begin{bmatrix} c & -s \\ s & c \end{bmatrix} \quad \text{in } d = 2, \quad (\text{A2a})$$

$$\mathbb{R} = \begin{bmatrix} c^2 + s^3 & cs & cs^2 - cs \\ cs & -s & c^2 \\ cs^2 - cs & c^2 & c^2s + s^2 \end{bmatrix} \quad \text{in } d = 3, \quad (\text{A2b})$$

where  $c = \cos \theta$  and  $s = \sin \theta$ . We choose  $\theta = \pi/7$  for all our calculations. For the calculations of the conductance of an open system connected with leads, we use the free boundary condition in transverse directions, and hence the phase factor in the hopping term of Eq. (A1) can be gauged away. To compare the open-system conductance with that of the closed one, we consider the Hamiltonian again without the phase factor in the hopping to calculate the Thouless conductance. We note that, for the above transport setup, and for a finite system, the real-space-momentum space duality of the model Eq. (A1) [27] is lost. For each finite system with linear dimension  $L$  under periodic boundary conditions we can generate a self-dual approximation [27]. This recipe is not applicable, however, for the transport setup. All the data points for the quasiperiodic system, shown here and in the Supplemental Material [32], are results of averaging over 300–400 values of  $\phi \in [0, 2\pi)$ , and we checked the convergence of our data for several parameter values with a larger number ( $\sim 1000$ – $2000$ ) of  $\phi$  averages.

- [1] E. Abrahams, P. W. Anderson, D. C. Licciardello, and T. V. Ramakrishnan, Scaling Theory of Localization: Absence of Quantum Diffusion in Two Dimensions, *Phys. Rev. Lett.* **42**, 673 (1979).  
 [2] P. W. Anderson, Absence of diffusion in certain random lattices, *Phys. Rev.* **109**, 1492 (1958).

- [3] S. Aubry and G. André, Analyticity breaking and anderson localization in incommensurate lattices, *Ann. Israel Phys. Soc.* **3**, 18 (1980).  
 [4] B. Simon, Almost periodic Schrödinger operators: A Review, *Adv. Appl. Math.* **3**, 463 (1982).

- [5] J. B. Sokoloff and J. V. José, Localization in an Almost Periodically Modulated Array of Potential Barriers, *Phys. Rev. Lett.* **49**, 334 (1982).
- [6] D. J. Thouless and Q. Niu, Wavefunction scaling in a quasi-periodic potential, *J. Phys. A: Math. Gen.* **16**, 1911 (1983).
- [7] M. Kohmoto, L. P. Kadanoff, and C. Tang, Localization Problem in One Dimension: Mapping and Escape, *Phys. Rev. Lett.* **50**, 1870 (1983).
- [8] M. Kohmoto, Metal-Insulator Transition and Scaling for Incommensurate Systems, *Phys. Rev. Lett.* **51**, 1198 (1983).
- [9] S. Ostlund, R. Pandit, D. Rand, H. J. Schellnhuber, and E. D. Siggia, One-Dimensional Schrödinger Equation with an Almost Periodic Potential, *Phys. Rev. Lett.* **50**, 1873 (1983).
- [10] S. Ostlund and R. Pandit, Renormalization-group analysis of the discrete quasiperiodic Schrödinger equation, *Phys. Rev. B* **29**, 1394 (1984).
- [11] J. B. Sokoloff, Unusual band structure, wave functions and electrical conductance in crystals with incommensurate periodic potentials, *Phys. Rep.* **126**, 189 (1985).
- [12] M. Schreiber, S. S. Hodgman, P. Bordia, H. P. Lüschen, M. H. Fischer, R. Vosk, E. Altman, U. Schneider, and I. Bloch, Observation of many-body localization of interacting fermions in a quasirandom optical lattice, *Science* **349**, 842 (2015).
- [13] A. Purkayastha, A. Dhar, and M. Kulkarni, Nonequilibrium phase diagram of a one-dimensional quasiperiodic system with a single-particle mobility edge, *Phys. Rev. B* **96**, 180204(R) (2017).
- [14] A. Purkayastha, S. Sanyal, A. Dhar, and M. Kulkarni, Anomalous transport in the Aubry-André-Harper model in isolated and open systems, *Phys. Rev. B* **97**, 174206 (2018).
- [15] V. K. Varma, C. de Mulatier, and M. Žnidarič, Fractality in nonequilibrium steady states of quasiperiodic systems, *Phys. Rev. E* **96**, 032130 (2017).
- [16] V. Khemani, D. N. Sheng, and D. A. Huse, Two Universality Classes for the Many-Body Localization Transition, *Phys. Rev. Lett.* **119**, 075702 (2017).
- [17] W. De Roeck and F. Huveneers, Stability and instability towards delocalization in many-body localization systems, *Phys. Rev. B* **95**, 155129 (2017).
- [18] I.-D. Potirniche, S. Banerjee, and E. Altman, Exploration of the stability of many-body localization in  $d > 1$ , *Phys. Rev. B* **99**, 205149 (2019).
- [19] F. Evers and A. D. Mirlin, Anderson transitions, *Rev. Mod. Phys.* **80**, 1355 (2008).
- [20] P. W. Anderson, D. J. Thouless, E. Abrahams, and D. S. Fisher, New method for a scaling theory of localization, *Phys. Rev. B* **22**, 3519 (1980).
- [21] B. L. Al'tshuler, Fluctuations in the extrinsic conductivity of disordered conductors, *Pis'ma Zh. Eksp. Teor. Fiz.* **41**, 530 (1985) [*JETP Lett.* **41**, 648 (1985)].
- [22] P. A. Lee and A. D. Stone, Universal Conductance Fluctuations in Metals, *Phys. Rev. Lett.* **55**, 1622 (1985).
- [23] P. A. Lee and D. S. Fisher, Anderson Localization in Two Dimensions, *Phys. Rev. Lett.* **47**, 882 (1981).
- [24] J. L. Pichard and G. Sarma, Finite-size scaling approach to anderson localisation. ii. quantitative analysis and new results, *J. Phys. C* **14**, L617 (1981).
- [25] A. MacKinnon and B. Kramer, The scaling theory of electrons in disordered solids: Additional numerical results, *Z. Phys. B* **53**, 1 (1983).
- [26] K. Slevin, P. Markoš, and T. Ohtsuki, Reconciling Conductance Fluctuations and the Scaling Theory of Localization, *Phys. Rev. Lett.* **86**, 3594 (2001).
- [27] T. Devakul and D. A. Huse, Anderson localization transitions with and without random potentials, *Phys. Rev. B* **96**, 214201 (2017).
- [28] D.-L. Deng, S. Ganeshan, X. Li, R. Modak, S. Mukerjee, and J. H. Pixley, Many-body localization in incommensurate models with a mobility edge, *Ann. Phys.* **529**, 1600399 (2017).
- [29] S. Ganeshan, J. H. Pixley, and S. Das Sarma, Nearest Neighbor Tight Binding Models with an Exact Mobility Edge in One Dimension, *Phys. Rev. Lett.* **114**, 146601 (2015).
- [30] J. W. Kantelhardt, in *Mathematics of Complexity and Dynamical Systems*, Fractal and Multifractal Time Series, edited by R. A. Meyers (Springer, New York, 2011).
- [31] T. Tél, Fractals, multifractals, and thermodynamics, *Z. Naturforsch. A* **43**, 1154 (2014).
- [32] See Supplemental Material at <http://link.aps.org/supplemental/10.1103/PhysRevB.99.224204> for the details of the calculations of conductances and the multifractal analysis. The Supplemental Material includes Refs. [50–53].
- [33] J. T. Edwards and D. J. Thouless, Numerical studies of localization in disordered systems, *J. Phys. C* **5**, 807 (1972).
- [34] D. J. Thouless, Electrons in disordered systems and the theory of localization, *Phys. Rep.* **13**, 93 (1974).
- [35] P. W. Anderson and P. A. Lee, The Thouless conjecture for a one-dimensional chain, *Prog. Theor. Phys. Suppl.* **69**, 212 (1980).
- [36] D. Braun, E. Hofstetter, A. MacKinnon, and G. Montambaux, Level curvatures and conductances: A numerical study of the Thouless relation, *Phys. Rev. B* **55**, 7557 (1997).
- [37] A. L. Goldberger, L. A. Amaral, L. Glass, J. M. Hausdorff, P. Ch. Ivanov, R. G. Mark, J. E. Mietus, G. B. Moody, C. K. Peng, and H. E. Stanley, PhysioBank, PhysioToolkit, and PhysioNet: Components of a new research resource for complex physiologic signals, *Circulation* **101**, e215 (2000).
- [38] D. Dominguez, C. Wiecek, and J. V. Jose, Wave-function and resistance scaling for quadratic irrationals in Harper's equation, *Phys. Rev. B* **45**, 13919 (1992).
- [39] N. Macé, A. Jagannathan, and F. Piéchon, Fractal dimensions of wave functions and local spectral measures on the fibonacci chain, *Phys. Rev. B* **93**, 205153 (2016).
- [40] N. Macé, A. Jagannathan, P. Kalugin, R. Mosseri, and F. Piéchon, Critical eigenstates and their properties in one- and two-dimensional quasicrystals, *Phys. Rev. B* **96**, 045138 (2017).
- [41] A. Jagannathan, P. Jeena, and M. Tarzia, Nonmonotonic crossover and scaling behaviors in a disordered 1D quasicrystal, *Phys. Rev. B* **99**, 054203 (2019).
- [42] R. Landauer, Electrical resistance of disordered one-dimensional lattices, *Philos. Mag.* **21**, 863 (1970).
- [43] E. N. Economou and C. M. Soukoulis, Static Conductance and Scaling Theory of Localization in One Dimension, *Phys. Rev. Lett.* **46**, 618 (1981).
- [44] D. S. Fisher and P. A. Lee, Relation between conductivity and transmission matrix, *Phys. Rev. B* **23**, 6851 (1981).
- [45] A. Szabó and U. Schneider, Non-power-law universality in one-dimensional quasicrystals, *Phys. Rev. B* **98**, 134201 (2018).
- [46] H. P. Lüschen, P. Bordia, S. Scherg, F. Alet, E. Altman, U. Schneider, and I. Bloch, Observation of Slow Dynamics Near

- the Many-Body Localization Transition in One-Dimensional Quasiperiodic Systems, *Phys. Rev. Lett.* **119**, 260401 (2017).
- [47] R. Vosk, D. A. Huse, and E. Altman, Theory of the Many-Body Localization Transition in One-Dimensional Systems, *Phys. Rev. X* **5**, 031032 (2015).
- [48] A. C. Potter, R. Vasseur, and S. A. Parameswaran, Universal Properties of Many-Body Delocalization Transitions, *Phys. Rev. X* **5**, 031033 (2015).
- [49] S.-X. Zhang and H. Yao, Universal Properties of Many-Body Localization Transitions in Quasiperiodic Systems, *Phys. Rev. Lett.* **121**, 206601 (2018).
- [50] E. Akkermans, Twisted boundary conditions and transport in disordered systems, *J. Math. Phys.* **38**, 1781 (1997).
- [51] W. Zhou, Y. Dang, and R. Gu, Efficiency and multifractality analysis of CSI 300 based on multifractal detrending moving average algorithm, *Physica A* **392**, 1429 (2013).
- [52] P. Markoš, Numerical analysis of the anderson localization, *Acta Phys. Slov.* **56**, 561 (2006).
- [53] J. A. Verges, Computational implementation of the Kubo formula for the static conductance: Application to two-dimensional quantum dots, *Comput. Phys. Commun.* **118**, 71 (1999).